

Infrasound Measurements from Wind Turbines under Various Atmospheric Conditions

S. D'Amico T. Van Renterghem D. Botteldooren

Ghent University, WAVES research group, Technologiepark 126, 9052 Zwijnaarde-Gent, Belgium
SarahDAmico@UGent.be

ABSTRACT

Infrasound exposure has become a main cause of opposition towards new wind turbine projects. In order to assess its relevance, a long term measurement campaign at close distance from a wind turbine was conducted using a low-frequency microphone. An ad-hoc designed and validated wind-shielding dome was used to improve the signal-to-noise ratio in the infrasonic frequency range. The acoustic measurements were accompanied by air temperature profile measurements and high acquisition frequency wind measurements. The infrasound power spectral density spectra from the wind turbines have been related to different nacelle positions, mean-wind-speed, turbulence intensity and the temperature's vertical profile. The on-going study aims at assessing the dependency of the wind turbine infrasound intensity from atmospheric parameters.

1. INTRODUCTION

The need for renewable sources of energy is resulting in an increment in the construction of wind farms. While wind turbines have a good reputation as efficient devices for the generation of green energy, their noise emissions are often reported as the main negative impact on the environment. Health problems related to long-term noise exposure and the potentially long distances infrasound can propagate in the atmosphere are reasons for concern.

Infrasound from wind turbines have broadband and tonal components. Blade-tower interaction is addressed to be responsible for the tonal characteristics of wind turbine infrasound [1]. During its rotation, the blade encounters a region of velocity deficit in front of the tower, resulting in temporal change of the angle of attack. This generates acoustic emissions at the blade passing frequency. Broadband infrasound from wind turbines originates from the interaction between the turbulent eddies advected with the wind flow and the blades [2]. Especially the large eddies lead to sudden changes in the aerodynamic loading of the blade.

The scientific community agrees that the effect of wind turbine infrasound on human health is currently unclear. Infrasound exposure from wind turbines is typically lower than the threshold of hearing [3], while intrinsic human body pressure variations could create infrasound signals in the inner ear that are larger. Psychological factors are thought to have prominence on the genesis of annoyance and health disorders [4]. On the other hand, physiological studies on the sensitivity of the human ear have revealed that although infrasound is not able to generate a hearing sensation, it could still produce

neuronal signals whose impacts are unknown [5]. Furthermore, the studies on prolonged exposure to low intensity infrasound are still sparse [6].

Despite wind turbine infrasound and low frequency noise are often reported, methodological studies and long-time measurements of infrasound and low frequency noise from wind turbines are scarce. Moreover, the studies on the influence of different factors, as meteorological and inflow conditions on the generation of infrasound from wind turbines are very limited in scientific literature.

Measuring infrasound from wind turbines also presents difficulties. Infrasound emissions from wind power generators occur simultaneously with wind-induced microphone noise, masking wind turbine infrasound.

This paper studies infrasound from wind turbines in correlation with different inflow and atmospheric conditions. A wind shielding dome was used to improve the signal-to-noise ratio in the infrasonic frequency range whose development and assessment was discussed in previous work [7].

2. METHODOLOGY

2.1 Data acquisition

The measurement campaign at a wind farm in the Melle Campus of Ghent University started in September 2019 and is currently ongoing. The wind farm is composed of three Enercon wind turbines of 2 MW, each placed at 450 m from each other. The wind turbines are pitch regulated and have a hub height of 104 m and a rotor diameter of 82 m.

The area is characterized by fully flat agricultural terrain and some sparse buildings are located at a distance of 200 m from the microphone. A main motorway is at approximately 250 m from the microphone. Figure 1 illustrates the wind farm.



Figure 1. Measurement location

Measurements were taken at 120 m from the central wind turbine. Acoustic pressure fluctuations were

measured using a GRAS 46 AZ low frequency microphone and preamplifier that ensures linear response from 0.5 Hz. The microphone was used together with a Alix System single board computer for continuous recordings at 48 kHz. 57s continuous recordings were collected every minute. A GPS clock was used to synchronize the recordings every minute.

The microphone was equipped with rain protection and a 10-cm diameter wind screen. The microphone was covered by a previously designed wind-shielding dome to reduce the wind-induced microphone noise at infrasound in order to improve the signal-to-noise ratio [7]. The Svantek 30 A Class 1 acoustic calibrator was used to record 1 kHz, 94 dB acoustic signal for calibration; recording the calibration signal was repeated on a weekly basis.

The meteorological data were acquired at three different heights, at 2, 10 and 104 m height. A Gill WindMaster 3D sonic anemometer was used at 10 m height to acquire wind data at 20 Hz acquisition frequency, at a resolution of 0.01 m/s and 0.01°C. The anemometer provided instantaneous values of wind speed, wind direction, vertical component of wind speed, speed of sound and sonic temperature.

Data at 2 m height were provided by the Department of Physics of Ghent University and were acquired at the meteorological station at 40 m from the microphone. The data are 1 minute based. The data at 104 m height (hub height) were provided by the wind farm operator and are 10 minutes based. The data provided both meteorological data and wind turbine data. The meteorological data at 2 and 104 m height included mean wind speed, standard deviation of mean wind speed, wind direction and temperature. The data at 2 m height provided also humidity and precipitation, while the wind turbine data at hub height provided power, rotational speed and nacelle position.

Figure 2 illustrates a schematic of the set up while Figure 3 presents some pictures of the measurement instrumentation in the field.

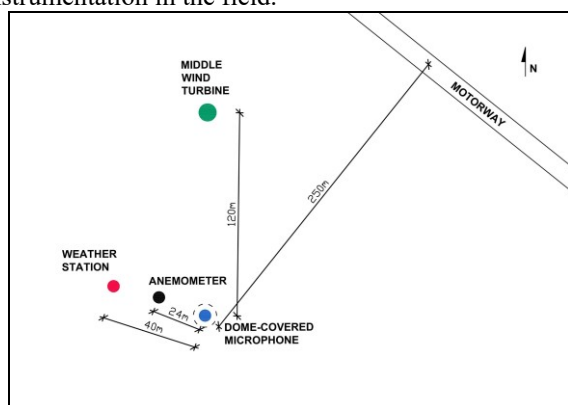


Figure 2. Schematic of the field measurement set up



Figure 3. Field measurement set up: sonic anemometer at 10 m height (left), wind-shielding dome covering the microphone (right, up) and the meteorological station (right, down)

2.2 Meteorological data processing

The meteorological data, as well as the wind turbine data were averaged over 10 minute-periods. The TI was calculated at the reference height (10 m). Wind sectors of 30° were assigned and the blade passing frequency was predicted from the rotational speed.

From the instantaneous data of the anemometer, the mean and fluctuating values of the three components of the instantaneous wind vector, as well as of the temperature scalar, were calculating using Reynolds decomposition on a 10 minute base. Friction velocity, turbulent kinetic energy, vertical turbulent heat flux and Monin-Obukhov length were calculated from the fluctuating values for each 10 minute at reference height.

In particular, the vertical turbulent heat flux is the mean value of the instantaneous product between the fluctuating part of the vertical wind speed component and of the fluctuating part of the temperature. Negative vertical turbulent heat flux indicates a stable atmosphere, while positive vertical turbulent heat flux indicates an unstable atmosphere.

Different mean wind speeds and temperature vertical profiles were also defined for each 10 minute based on the synchronized mean values at the three different heights

2.3 Acoustic data processing

From the recorded signals, rainy period were excluded, as well as reported period with disturbing noises in the proximity of the microphones.

For each of the 57s signal, the wave signal was first calibrated with the root-mean-square (rms) of the 94 dB signal at 1kHz. The signal were then corrected for the internal filter of the Alix System at infrasound.

The PSDs were calculated from each 57s signal. For each 10 minutes, the PSDs were linearly averaged and synchronized with the meteorological data. The PSD spectra were sorted for wind sector, mean wind speed, TI and turbulent vertical heat flux at reference height. For each group, the average power spectra density spectra were calculated.

3. RESULTS

Some preliminary results are presented in this section. The PSDs are presented for some of the different atmospheric conditions described in the previous sections. Figure 4 presents the averaged PSD spectra from the wind farm measured by the microphone for mean wind speeds from 2 to 7 m/s.

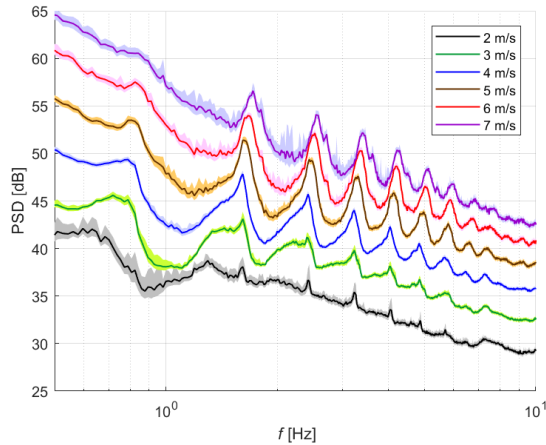


Figure 4. PSD mean spectra for different mean wind speed. The 95 % confidence intervals are calculated with the bootstrapping method, assuming no specific statistical distribution of the data, and are depicted as shaded areas

The PSD spectra from the wind farm increase with increasing mean wind speed. The blade passing frequency is visible for the cases from 3 to 6 m/s mean wind speed. The blade passing frequency becomes submersed in the wind-induced microphone noise for 7 m/s mean wind speed. The subsequent harmonics, however, can be clearly identified in all of the cases.

The dependency of the PSD from nacelle position are evaluated in Figure 5. For different mean wind speeds, the PSD for different 30° nacelle-position sectors are compared.

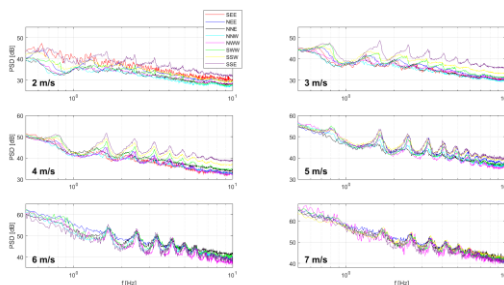


Figure 5. PSD mean spectra for different 30° nacelle-position sectors for mean wind speeds from 2 to 7 m/s

The mean PSD spectra present a significant variability with nacelle position at infrasound frequencies. The sectors where the higher PSD spectra are measured are those where the microphone is in the cross-direction with respect to the wind turbines. This could suggest a modulation effect also at very low frequencies.

The results are further analyzed to evaluate the influence of the turbulence content on the infrasound

emission from the wind farm. Figure 6 presents the six mean wind speed cases for different TIs.

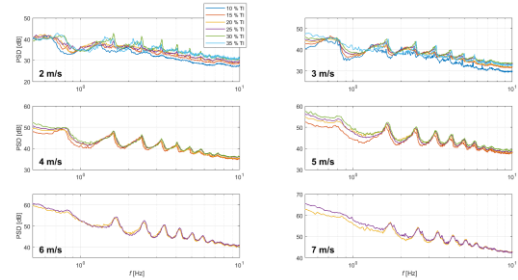


Figure 6. PSD mean spectra for different TIs for mean wind speeds from 2 to 7 m/s

For 2 and 3 m/s mean wind speed, both the broad band component of the PSD spectra and the blade passing frequency see an increase with increasing TI. In particular, the blade passing frequency (BPF) peaks and their harmonics become more pronounced as the turbulent content in the wind flow increases. For the higher mean wind speeds instead, the wind turbine acoustic peaks remain almost constant with increasing TIs. Differently, the broadband noise between the peaks, especially in the lowest range of the showed spectra, increases for higher TIs.

In the lowest range of the infrasound spectra, there is a non-negligible contribution from the wind-induced microphone noise which partly covers the BPF and that depends on TIs.

Figure 6 shows the PSDs for different mean wind speeds for the cases of stable and unstable meteorological conditions.

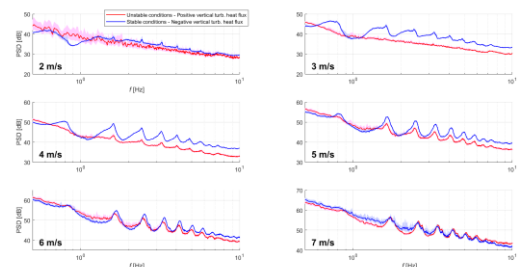


Figure 7. PSD mean spectra for stable and unstable atmosphere for the different mean wind speeds. The 95 % confidence intervals are calculated with the bootstrapping method, assuming no specific statistical distribution of the data, and are depicted as shaded areas

Figure 7 illustrates the PSDs for different mean wind speeds in stable and unstable atmospheric conditions. The stable and unstable conditions are defined by the turbulent vertical heat flux. For low mean wind speeds, the difference between wind turbine immissions in stable and unstable conditions is significant. For unstable conditions and low mean wind speeds it is not possible to identify the wind turbine peaks while these are clear for stable conditions. For higher mean wind speeds, the difference is less and the peaks are clear in both meteorological conditions.

Figures 8 and 9 present the acoustic spectrograms for two different days together with the instantaneous wind spectrograms and the trends of the mean wind speed at reference height (MWS), the wind turbine power (Power), the nacelle position (N. pos), presented as a sinusoidal function and of the vertical turbulent heat flux (Turb. h. flux). The two consecutive days, (2/9/2019 in Fig. 8 and 3/9/2019 in Fig. 9) present two different situations. In Figure 8 there is a predominance of broad band noise while in Figure 9 the tonal components are predominant.

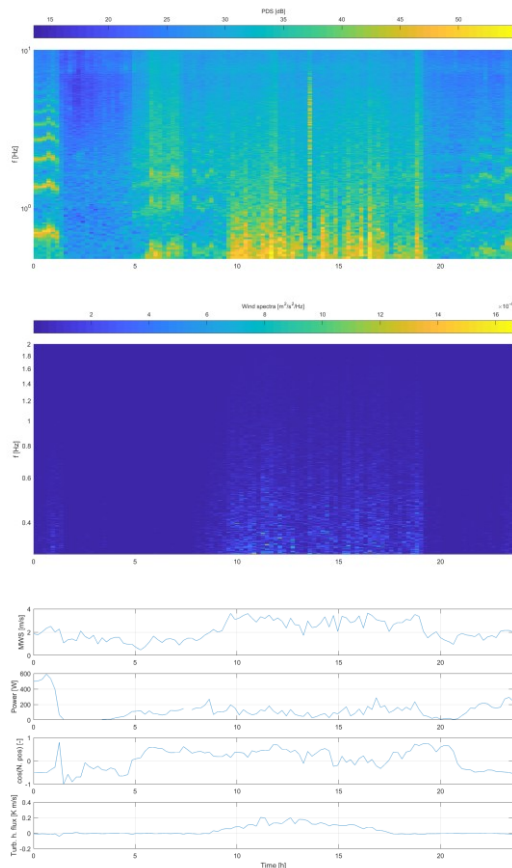


Figure 8. Acoustic spectrogram (upper), instantaneous wind spectrogram (middle), MWS, wind turbine power, Nacelle position and vertical turbulent heat flux trends (lower) for 10 minutes resolution for 2nd September 2019

In the acoustic spectrogram in Figure 8, infrasound broadband noise can be seen in the temporal window between h. 10 and 19. Tonal components from the wind turbines can be clearly seen mainly in the first hour and a half. In Figure 9, the tonal components of the wind turbines are present almost the whole day. Only between h. 12 and 16 the tonal components are not visible and the broad band noise dominates.

Especially the broad band noise is strongly correlated with the highest values in the instantaneous wind spectrogram which indicates a stronger energetic content in the fluctuating velocity. The broad band noise correlates also with a higher mean wind speed and positive vertical turbulence heat flux.

The tonal components results to be strongly dependent on the power production of the wind turbines and are more visible with negative vertical turbulent heat flux conditions.

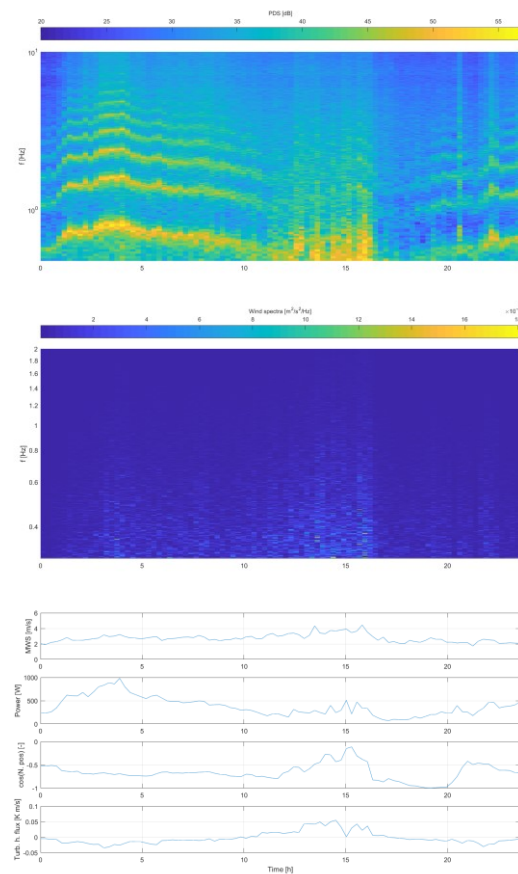


Figure 9. Acoustic spectrogram (upper), instantaneous wind spectrogram (middle), MWS, wind turbine power, Nacelle position and vertical turbulent heat flux trends (lower) for 10 minutes resolution for 3rd September 2019

The tonal components visible in the measurements can be clearly attributed to the BPFs of the wind turbines and their harmonics while the broad band noise seems to be determined by the energy in the wind, suggesting that this could be attributed to wind induced noise at the microphone. The spectrograms, together with the meteorological trends can help in correctly identify the wind turbines infrasound immissions.

4. CONCLUSIONS

A long-term measurement campaign was carried out, using a low-frequency microphone and a wind-shielding dome to identify immissions from wind turbines in the infrasonic frequency range. An extensive and detailed collection of meteorological data was measured.

The preliminary analysis allowed to identify the infrasound from wind turbines for different mean wind speeds, turbulence intensities and meteorological conditions. The blade passing frequency is clearly visible for low mean wind speeds. The wind turbine peaks can be

clearly identify and show to be constant for different TI conditions. The broad band noise shows an increase with TI and a correlation with high energy in the wind and unstable atmospheric conditions. Stable atmospheric conditions results more critical for wind turbine immissions at least at low mean wind speeds.

5. REFERENCES

- [1] G. Van den Berg: "The beat is getting stronger: the effect of atmospheric stability on low frequency modulated sound of wind turbines," *Journal of Low Frequency Noise, Vibration and Active Control*, Vol. 24, No. 1, pp. 1–24, 2005.
- [2] S. Wagner, R. Bareiss, G. Guidati: *Wind turbine noise*, Springer, Berlin, 1996.
- [3] I. van Kamp, F. van den Berg: "Health Effects Related to Wind Turbine Sound, Including Low-Frequency Sound and Infrasound," *Acoustics Australia*, Vol. 46, No. 1, pp. 31–57, 2018.
- [4] G. Leventhal: "Infrasound at the ear," *Proceedings of the 5th International Conference on Wind Turbine Noise*, 2013.
- [5] A. N. Salt, T. E. Huller: "Response of the ear to low frequency sound, infrasound and wind turbines," *Hearing Research*, Vol. 268, No. 1-2, pp. 12–21, 2010.
- [6] C. Balatsas, I. van Kamp, R. Poll, J. Yzermans: "Health effects from low frequency noise and infrasound in the general population: It is time to listen? A systematic review of observational studies," *The Science of the Total Environment*, Vol. 557-558, pp. 163-169, 2016.
- [7] S. D'Amico, T. Van Renterghem, D. Botteldooren: "Measuring infrasound from wind turbines: the benefits of a wind-shielding dome," *Proceedings of the 8th International Conference on Wind Turbine Noise*, 2019.